



Site Amplification Characteristics with Soil Nonlinearity Observed in K-NET and KiK-net and Their Empirical Modeling

Ziqian Wang⁽¹⁾ and Hiroshi Kawase⁽²⁾

⁽¹⁾ Graduate Student, Department of Architecture and Architectural Engineering, Kyoto University, Kyoto, Japan, ou.jiken.55e@st.kyoto-u.ac.jp

⁽²⁾ Program-Specific Professor, DPRI, Kyoto University, Kyoto, Japan, kawase@sere.dpri.kyoto-u.ac.jp

Abstract

The Horizontal-to-Vertical spectral ratio method (the HVR method) was proposed as a direct substitute for S-wave amplification by Nakamura [1]. Noguchi and Sasatani [2] found that the HVR of earthquake (EHVR) will be changed when soil nonlinearity occurs and proposes an index to see the degree of nonlinearity. With the diffuse field concept we recently found that the EHVR is the ratio of the S-wave transfer function with respect to the P-wave transfer function with vertical incidence from the seismological bedrock with a coefficient for HVR at the bedrock. Then if we do not have significant nonlinearity in the P-wave transfer function during the strong shaking, we will see soil nonlinearity on the EHVR as the nonlinearity of the S-wave amplification. In this study, we tried to find the difference between the EHVR with soil nonlinearity and those without, quantify the difference, and utilize it to correct the linear S-wave amplification for improving the result of strong motions prediction in the near field.

Firstly, we found that the difference between EHVR with and without soil nonlinearity could be regarded as a shift in frequency and/or amplitude. We picked up the peak frequencies for all the earthquake records observed at several selected sites in southwestern Japan and plotted them as a function of PGA (Peak Ground Acceleration) to see the shift. We found that the threshold of peak frequency decreasing in terms of PGA is 50 cm/s^2 .

Secondly, we defined two coefficients, alpha and beta, as the shift due to nonlinearity on the frequency and amplitude by using strong motion records observed by K-NET and KiK-net in southwestern Japan, defined as the DoD (Degree of Difference) to judge the matching between the observed EHVR with soil nonlinearity and reproduced EHVR from alpha and beta and the EHVR in a linear regime. Based on the DoD, we obtained two empirical relationships, namely, alpha-PGA and beta-PGA.

Thirdly, once we obtained the coefficients alpha and beta from our empirical relationships for PGA, we reproduced the estimated EHVR with soil nonlinearity from the averaged EHVR for small PGA recordings without soil nonlinearity. Based on the individual nonlinear EHVR calculated from the single strong-motion, together with the averaged EHVR, we obtained velocity structure with and without soil nonlinearity by Nagashima et al.'s Program [3]. Then, we confirmed that the observed linear and nonlinear EHVRs can be reproduced by the inverted velocity structures.

Fourthly, we utilized the VACF (Vertical Amplification Correction Function) method [4] and the DYNEQ Program [5] to obtain HSAF (Horizontal Site Amplification Factor). We compared these HSAFs obtained by four methods to verify the application of our empirical relationships.

As described, we obtained two empirical relationships between the frequency shift with PGA and the amplitude shift with PGA. Nowadays theoretical prediction of soil amplification considering nonlinearity can be made through the time-domain nonlinear analysis of soil layers, however, in such theoretical methods, we need detailed velocity information down to the seismological bedrock and nonlinear properties of sediments, which are difficult to obtain in a wider area for a scenario-type seismic risk evaluation. The proposed method has a wider applicability and is easier to use than the theoretical methods, without knowing the detailed information of soft sediments.

Keywords: Site amplification factor, The HVR method, Soil nonlinearity, Horizontal-to-Vertical spectral ratio



1. Introduction

The investigations about site amplification factors have been going on for decades. In general, the site amplification factor was defined as a seismic waveform amplification factor from a certain subterranean layer to the earth's surface. The site amplification factors depend on the S-wave velocity of the soil layers, the density of soil, internal damping of the layers, and composition of the soil layers. Shima [6] proposed that it is almost a linear relationship between the analytically calculated site amplification at a site and the ratio of the S wave velocity near the earth's surface to the S-wave of the seismic bedrock, although the intermediate layers are different. Furthermore, Finn [7] proposed that the nonlinear soil effect on the site amplification during the strong motion has to be considered. Later, Kawase and Matsuo [8] and Kawase [9] utilized the GIT (Generalized spectral inversion technique) method to separate the source, path, and site amplification factors from the data of K-NET and KiK-net and JMA Shindokeyi network in Japan successfully. About the evaluation of the nonlinear site response, Wen et al. [10] proposed the EHVR of S-wave on the earth's surface could be regarded as an indicator of soil nonlinearity. Then, Noguchi et al. [2] defined an index named DNL (The degree of nonlinearity) as a function to quantify the difference between EHVR of weak motions and EHVR of strong motions. The EHVR of weak motions stands for the linear case, and the EHVR of strong motion can stand for the nonlinear case.

In this study, we not only quantified the degree of difference between the EHVR considering the linear soil behavior with EHVR considering the nonlinear soil behavior but also reproduced pseudo EHVR considering soil nonlinearity. Then, by the simulation or direct calculation from either Nagashima et al.'s Program [3], DYNEQ [5], VACF (Vertically Amplification Correction Function) method, VHbR method, or VACF-NCF method (Vertically Amplification Correction Function & Nonlinearity Correction Function hybrid method), we obtained the site amplification factors considering soil nonlinearity and compared them with each other.

2. The DoD (Degree of Difference) for soil nonlinearity

2.1 Sites & Data

In this study, we selected total of 119 sites, which recorded strong motions more than 70 cm/s^2 in terms of PGA from Kinki area in the southwestern Japan. The selected sites were shown in Fig.1. To avoid a disturbance from soil nonlinearity, we selected first the records in which PGA is from 4 to 15 cm/s^2 to ensure what we obtained are in the linear regime. Here, the PGA means the largest acceleration of north-south acceleration, west-east acceleration.

To avoid an intense influence of surface waves, we only utilized the weak motions in which epicenter distances are less than 150 km. We also checked each waveform by sight to ensure there is not a significant influence of surface waves on the waveform. Another selection is the date of the recorded earthquake. We selected the data from 2000 to 2019 in most of the sites. However, in some sites, EHVRs have a significant difference after 2001, 2004, or 2007. In that case, we selected a part of the data from 2000-2019. Table 1 shows the particular sites and the selected durations in those sites.

Table 1 – Selected years of data in particular sites

Sites	HYGH03	HYGH04	HYGH05	HYGH06	HYGH07	HYGH09	HYGH11	HYGH12
Years	2008-2017	2008-2018	2001-2005	2012-2016	2008-2016	2008-2018	2009-2018	2009-2018
Sites	HYGH13	NARH01	NARH03	NARH04	NARH05	NARH06	NARH07	
Years	2016	2001-2006	2008-2018	2008-2014	2001-2007	2008-2018	2009-2018	

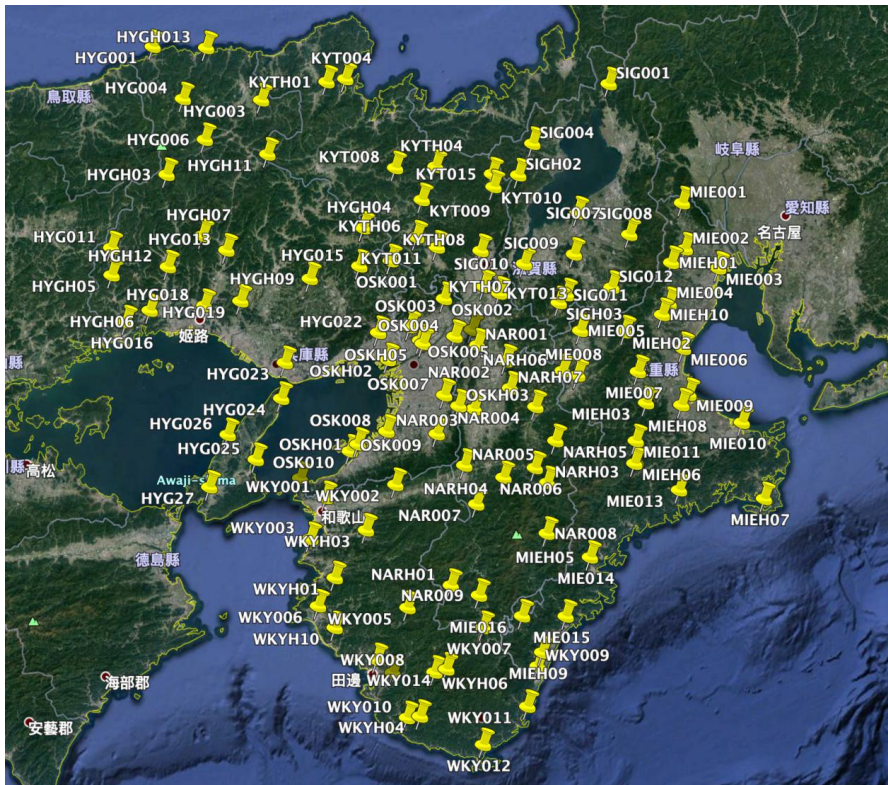


Fig. 1 – Sites selection (on top of the map from Google Earth, 2019)

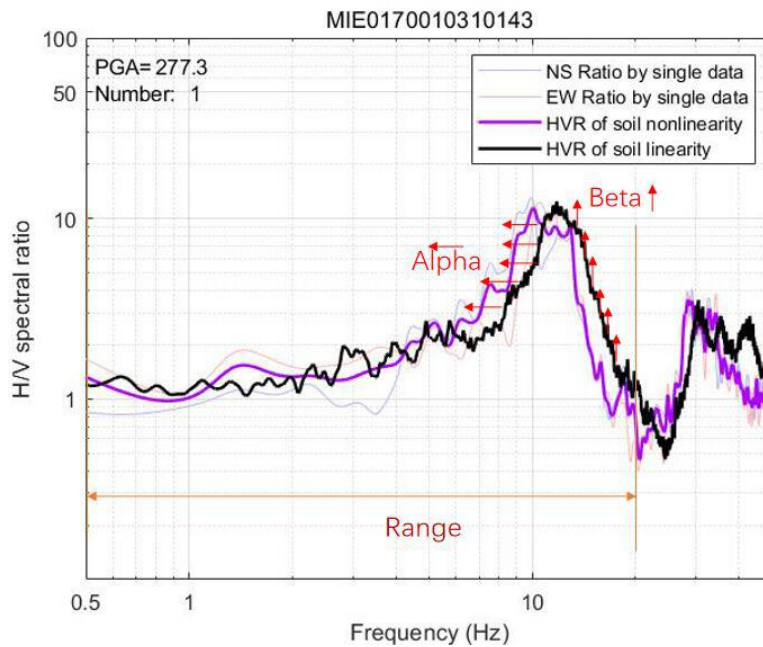


Fig. 2 – Soil linear EHVR & Soil nonlinear EHVR

2.2 Degree of difference

As an example in Fig.2 showed, the purple line is a nonlinear EHVR of one record, whose PGA was 277.3 cm/s². The black line is a linear EHVR calculated as an averaged value over several weak motions at MIE017 site. For EHVRs RMS (root mean squared) values of two horizontal components are used throughout this paper. We found a systematic difference between the purple line (the nonlinear EHVR) and



the black line (the linear EHVR) clearly, and we proposed that the difference could be regarded as a shift of EHVR from linearity to nonlinearity, and these shifts exist in both the frequency axis (X-axis) and the amplitude axis (Y-axis).

To quantify the shift between nonlinear and linear EHVRs, we proposed Eq. (1). Here n is the number of frequency data of EHVR, c is a coefficient to balance the weight, f is frequency, $EHVR_{lin}$ is the linear EHVR, $EHVR_{non}$ is the nonlinear EHVR, alpha and beta are two variables, which can influence DoD in the frequency and the amplitude.

$$DoD = \frac{|\sum_{i=1}^n c \cdot \log \frac{e^{EHVR_{lin}(f(i) \cdot 10^\alpha)} \cdot 10^\beta}{e^{EHVR_{non}(f(i))}}|}{n} \quad (1)$$

If we used Fig. 2 to explain Eq. (1), alpha could be regarded as a shift in the frequency axis from the linear EHVR to the nonlinear EHVR, beta could be regarded as a shift in the amplitude axis from the linear EHVR to the nonlinear EHVR. The value of DoD could be regarded as an averaged amplitude difference, which has already been transformed into the logarithmic coordinate system.

By changing the values of alpha and beta, we can obtain a figure like Fig. 3. The bright color means the DoD is large, and the deep color means DoD is small. The red point in Fig. 3 means that when alpha is equal to 0.05, and beta is equal to -0.01, the DoD, which is equivalent to 0.16, is minimum. Due to the DoD is an averaged amplitude difference, the smallest DoD means the difference is smallest, and also implies the matching between the linear EHVR and the nonlinear EHVR is best. The alpha and beta in this best matching case is treated as a piece of data to help us finish Fig.5 and Fig.6.-

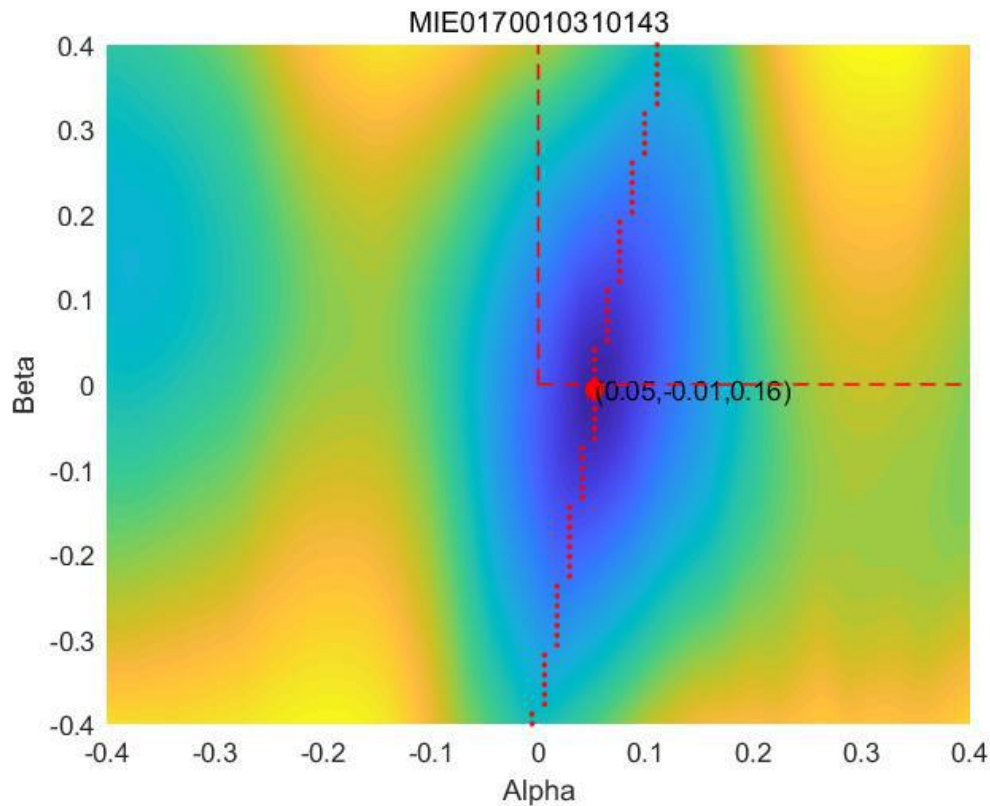


Fig. 3 – The different values of DoD by changing alpha and beta

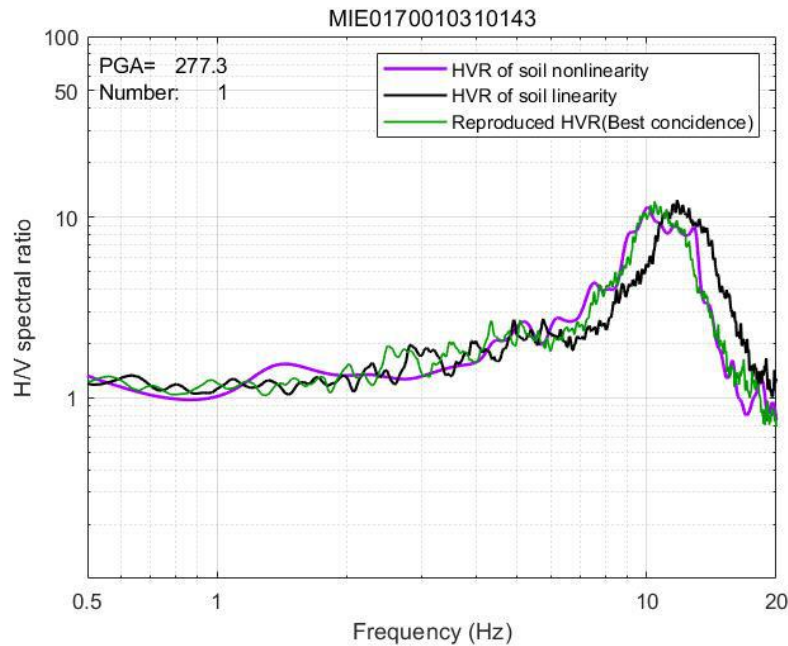


Fig. 4 – Soil linear EHVR, nonlinear EHVR and reproduced EHVR

In the example in Fig. 4, the black line is an averaged linear EHVR, the purple line is a nonlinear EHVR, and the green line is a reproduced nonlinear EHVR from the black line (The linear EHVR) with the obtained alpha and beta in the best matching case. This figure shows that after we calculated the alpha and beta in the best matching case, we moved the linear EHVR (The black line) by this alpha and beta in the frequency axis and the amplitude axis to obtain the reproduced EHVR (The green line). Due to the reproduced EHVR and the nonlinear EHVR are very similar, we regarded the alpha and beta in the best matching case as the real shift from the linear EHVR to the nonlinear one, and we named this alpha and this beta as α_s and β_s .

After we utilized more than 7,000 pieces of data from Kinki-area for calculating their α_s and β_s , we obtained two empirical figures. They are Fig. 5 and Fig. 6. We should note that the significant nonlinearity can be seen only those records with PGA higher than 100 cm/s^2 and that β_s becomes positive in that nonlinear regime on the average, meaning higher amplification than the linear regime.

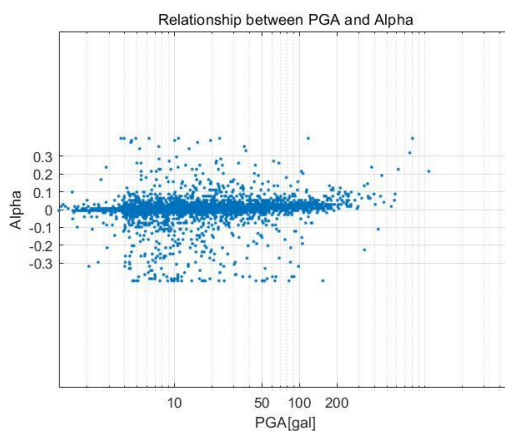


Fig. 5 – The relationship between α_s and PGA

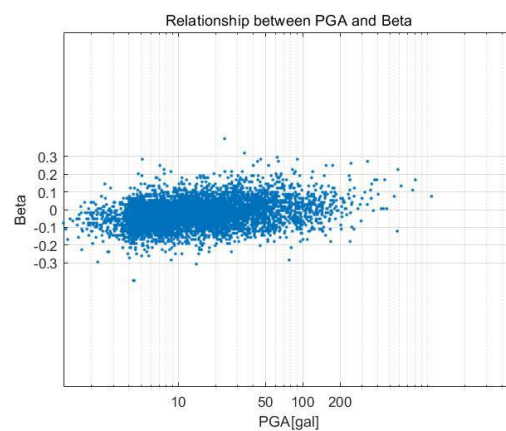


Fig. 6 – The relationship between β_s and PGA



2.3 Nonlinearity correction function (NCF)

In this study, because we assumed that nonlinear response would happen when PGA exceeded 100 cm/s², we only utilized the data whose PGA exceeds 100 cm/s² to fit a curve by parabolic function. We obtained Eq. (2) and Eq. (3) after fitting. We showed the utilized data and the parabolic curves of Eq. (2) and Eq. (3) in Fig. 7 and Fig. 8.

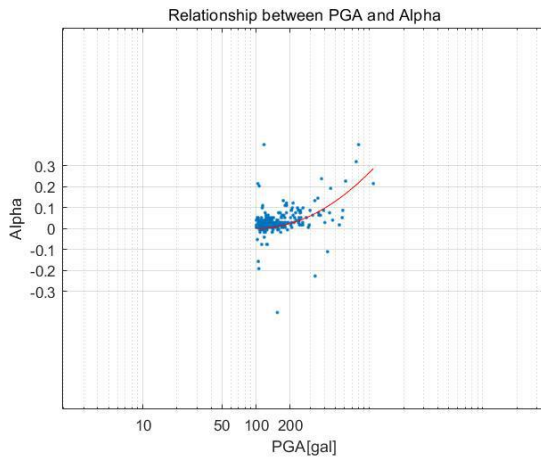


Fig. 7 – The parabolic function about α_s

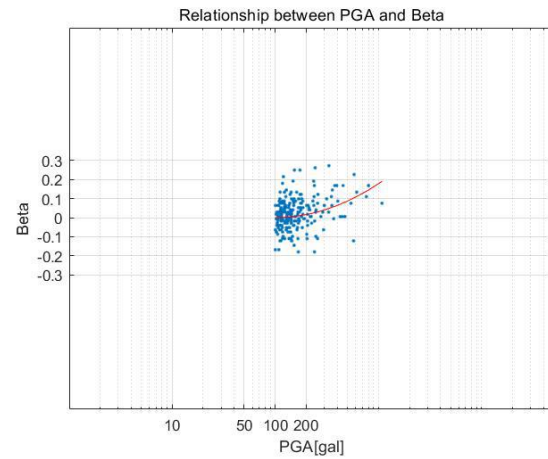


Fig. 8 – The parabolic function about β_s

$$(2) \quad \alpha_s = 0.2668 \cdot (\log_{10}PGA - 2)^2$$

$$(3) \quad \beta_s = 0.1773 \cdot (\log_{10}PGA - 2)^2$$

After that, we defined $f_c(i)$ and $a_c(i)$, $f_c(i)$ is the frequency of corrected EHVR on the i point and $a_c(i)$ is the amplitude of corrected EHVR on the i point, which can be modeled by $f(i)$, the frequency of initial EHVR on the i point and $a(i)$, the amplitude of initial EHVR on the i point, as follows:

$$(4) \quad f_c(i) = f(i) \cdot 10^{\alpha_s}$$

$$a_c(i) = a(i) \cdot 10^{\beta_s} \quad (5)$$

We named Eq. (2), Eq. (3), Eq. (4) and Eq. (5) as NCF (Nonlinearity Correction Function). The correction by NCF means that if we have a predicted PGA, we can obtain relevant α_s and β_s . Then, we can modify the averaged linear EHVR to reproduce predicted nonlinear EHVR by α_s and β_s .

Fig. 9 is an example to show the reproduced EHVR by NCF; the purple line is a single nonlinear EHVR by a single recorded earthquake data. In Fig. 9, the utilized earthquake data is 'MIE0170010310143'. The black line is the averaged linear EHVR at MIE017. The green line is the reproduced EHVR based on the best matching, in other words, based on the smallest DoD. The blue line is the corrected EHVR based on NCF. The blue line is very close to the green line and so it is very difficult to distinguish to each other. This means that our estimated EHVR by NCF is very similar to the estimated EHVR based on the smallest DoD and hence the observed EHVR with nonlinearity. That is what we expect to find, and it shows that NCF is appropriate to utilize to obtain nonlinear EHVRs empirically. However, we should note that there are significant scatters in the individual values of corrections as shown in Figs. 7 and 8. We should accept these degree of deviation in our average prediction of NCF.

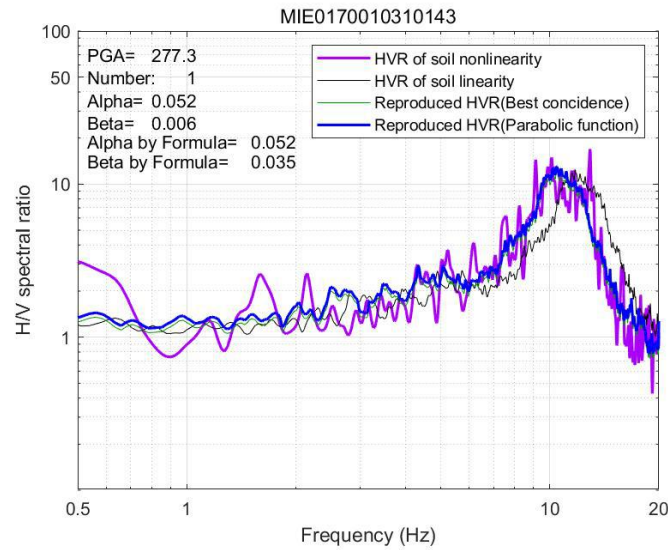


Fig. 9 – Four types of EHVR to compare in the nonlinear regime.

3. Velocity inversion considering and linear and nonlinear soil behavior

We performed the S-wave velocity inversion considering soil linearity and soil nonlinearity by Nagashima et al.'s Program based on the HHS method [3]. The calculation flow chart of Nagashima et al.'s code is shown in Fig. 10. This program can calculate the theoretical EHVR automatically, calculate the difference between the theoretical EHVR and the observed EHVR, and find a model with the minimum misfit as the final theoretical EHVR. The equation of misfit is as follows:

$$\text{misfit} = \sum_{f_{\min}}^{f_{\max}} [HVR_{obs}(f) - HVR_{the}(f)]^2 \quad (6)$$

In this equation, f is the frequency, HVR_{obs} is the observed EHVR, HVR_{the} is the theoretical EHVR, f_{\min} is the minimum frequency, and f_{\max} is the maximum frequency.

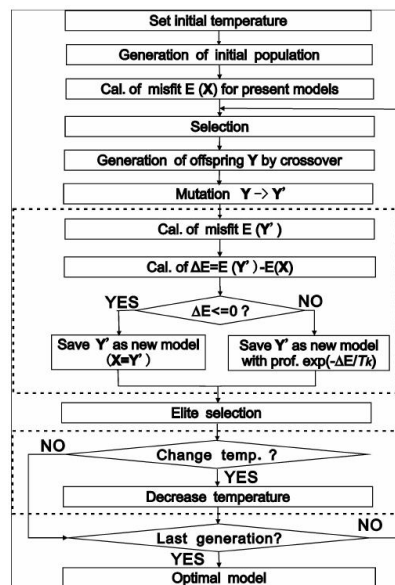


Fig. 10 – Calculation flow chart of HHS method [3]



Here we only showed an example to represent the velocity structure considering the soil linearity and soil nonlinearity. To perform DYNEQ [5] for horizontal site amplification factors, the S-wave velocity structure models considering both soil linearity and nonlinearity are necessary.

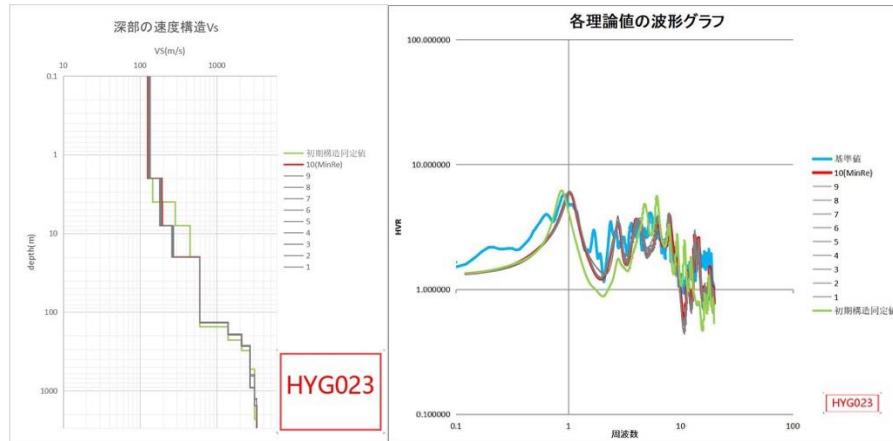


Fig. 11 – Velocity structure considering soil linearity the resultant EHVRs with the observed one.

As Fig. 11 showed, the left-hand panel is the linear S-wave velocity structure at HYG023 determined from the averaged EHVR for weak motions. The green line is the initial model before the inversion. At every site, the nine grey lines correspond to nine models of inversion with different initial genes, respectively, and the red line corresponds to the best inverted model, which has the minimum residual in Eq. (6). We chose the velocity structure corresponding to the red line as the initial velocity structure when we executed the nonlinear inversion. The right hand one is EHVRs of these velocity structures. The blue line is the averaged observed linear EHVR, which is the target of the inversion. The green line is the HVR calculated from the initial model before the inversion.

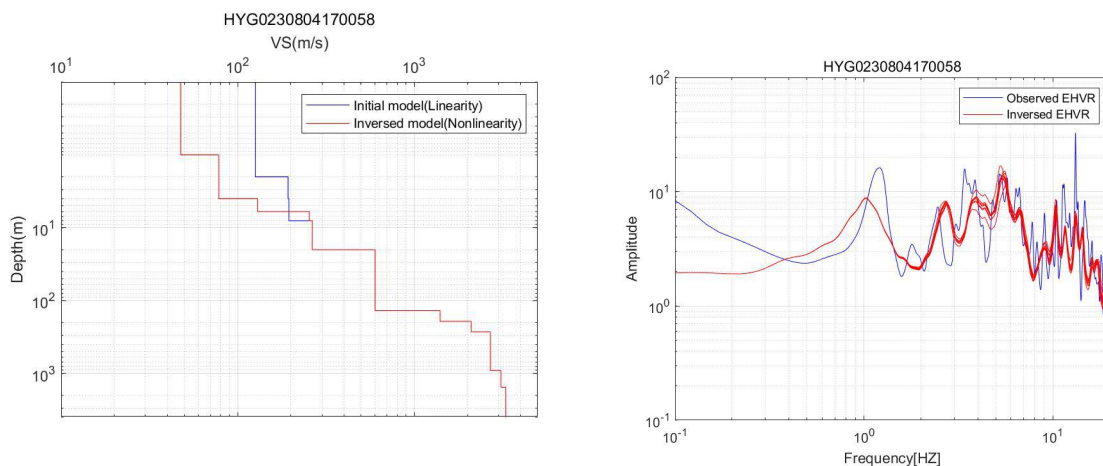


Fig. 12 – The velocity structure considering soil nonlinearity and its EHVR with the observed.

As Fig.12 showed, the left-hand panel is the nonlinear velocity structure at HYG023 determined from the large PGA record, in comparison to the linear velocity structure in blue. Since the velocity structure depends on a strong individual motion with nonlinearity, we used only EHVR of the individual strong motion as a target to perform the inversion. In Fig.12, the left-hand one is the velocity structure. The blue line is the initial model for the nonlinear inversion, which is the best model in the linear inversion. The red line is the inversed nonlinear velocity model, which has a minimum residual from ten trials. In the right-hand panel, the red line are inversed EHVRs for ten trials. The blue line is observed EHVR calculated from an individual data named 'HYG0230804170058'. The observed EHVR is well reproduced by the inversion and



the inverted model from the high PGA record really showed the degradation of S-wave velocities in the shallower part less than 10 m.

4. Comparisons of site amplification factors

Kawase et al. [4] proposed ‘Double empirical corrections to Nakamura method’. They mentioned that the site amplification factor for the horizontal component (HH_bR) could be defined as:

$$HSAF = HH_bR = \frac{H_s}{H_b} = \left(\frac{H_s}{V_s} \right) * \left(\frac{V_s}{H_b} \right) = EHVR * VH_bR \quad (7)$$

In Eq. (7), H_s is the horizontal component spectra on the surface, V_s is the vertical component spectra on the surface, H_b is the horizontal bedrock input motion spectra. VH_bR is the amplification ratio of the V_s with respect to H_b . Because of the definition of HH_bR , HH_bR can be regarded as HSAF (Horizontal site amplification factor). Double empirical corrections, which is a widely applicable method, means they utilized the pseudo-EHVR and the empirical VH_bR for obtaining the pseudo- HH_bR . In this study, we utilized both the individual VH_bR calculated from site factors of vertical component in GIT [11, 12] and the empirical VH_bR calculated here in the same way as in Kawase et al. [4]. We named the latter empirical VH_bR , which is the averaged VH_bR from more than 1,600 sites in Japan, as VACF (Vertically Amplitude Correction Function) [13].

4.1 Comparisons of horizontal site amplification factors in the linear case

In the linear case, we calculated three types of HSAF (Horizontal Site Amplification Factor). As Fig.13 showed, the HSAF (Theory) is a theoretical horizontal site amplification factor. It is calculated by DYNEQ based on the 1-D multiple reflection theory. Here, we used the inversed velocity structure considering soil linearity, which we showed in Fig. 11, as the best S-wave velocity structure model. We obtained the site amplification factors from 30 sites, among which Fig. 13 is only one example to show results.

The HSAF ($EHVR * VH_bR$) is a close-to-exact observed HSAF from GIT. The EHVR is the averaged linear EHVR. The VH_bR is a ratio of vertical component spectra on the earth’s surface with respect to horizontal component spectra on the seismic bedrock. It is also calculated from GIT by Nakano et al. [11, 12]. The method, which we utilized to obtain the HSAF($EHVR * VH_bR$), means that we could obtain high-accurate site amplification factors even if we do not know the S-wave velocity structure once we perform GIT.

The pHSAF ($EHVR * VACF$) means the pseudo horizontal site amplification factor. The VACF, which calculated from Kawase et al. [13], is the averaged VH_bR from all sites in the database with ten or more records. The EHVR used here is the averaged linear EHVR. The VACF method is an empirical method to obtain site amplification factors. It means that we need not perform any estimations of S-wave velocity and rigorous velocity structure inversions. We could obtain site amplification factors anywhere, as long as we have the EHVR or pEHVR from microtremors at that location.

From Fig. 13, we noted that the HSAF(Theory), the HSAF($EHVR * VH_bR$), and the pHSAF ($EHVR * VACF$) are very similar to each other. They are incredibly similar in the tendency of descend and ascend, and their frequency peaks are very similar. The differences between their amplitudes are within acceptable limits. The results of comparisons noticed that as a very efficient method, the VACF method is very desirable and appropriate.

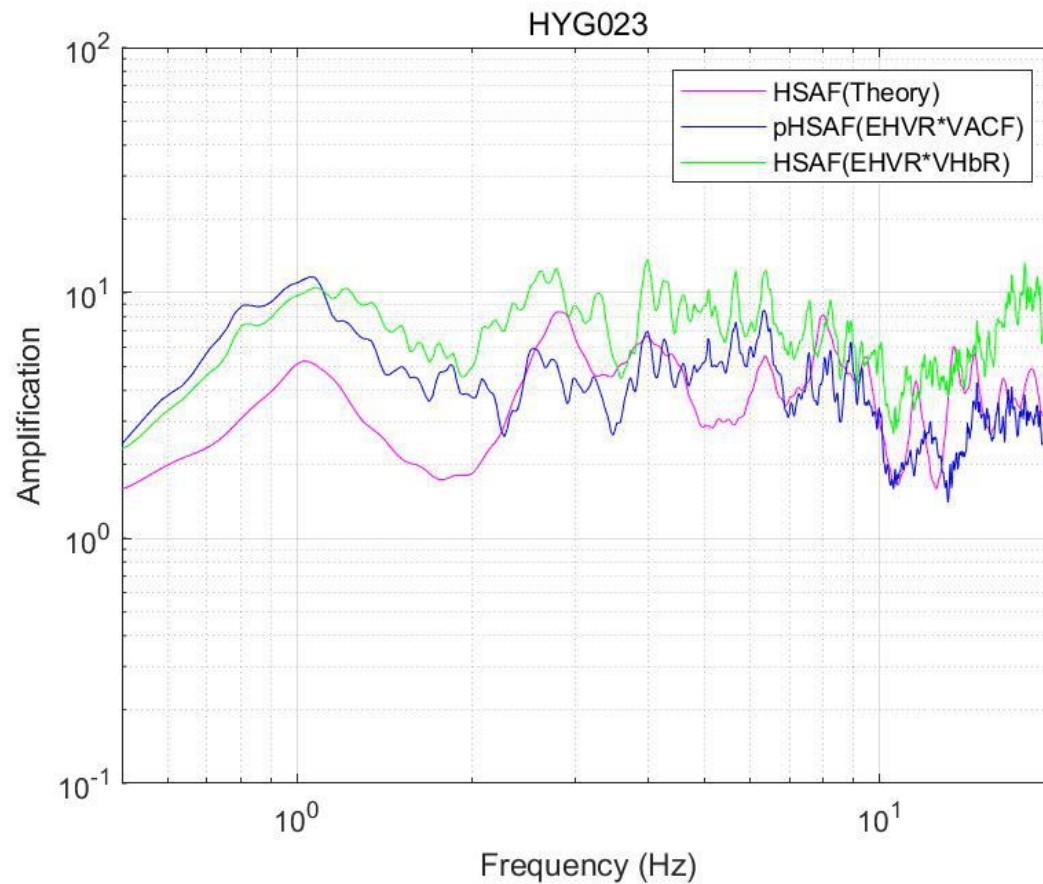


Fig. 13 – HSAF(Theory), pHSAF(EHVR*VACF), and HSAF (EHVR*VH_bR)

4.2 Comparisons of horizontal site amplification factors in the nonlinear case

In the nonlinear case, if we assumed that there would be negligible nonlinearity in the vertical component, we could regard that the value of nVH_bR (Nonlinear VH_bR) is the same as the value of VH_bR. As Fig. 14 showed, we calculated four types of HSAF considering soil nonlinearity. Fig.14 is an example. Actually, we obtained 68 site amplification factors considering soil nonlinearity from 68 pieces of strong motion data.

The nHSAF (Theory) is a theoretical nonlinear horizontal site amplification factor by DYNEQ. Here, we used the inverted velocity structure considering soil nonlinearity, which we showed in Fig. 12, as the S-wave velocity structure model deviated from the linear model. When we performed the nonlinear inversion, the target EHVR is a ratio from an individual strong motion with high PGA.

The nHSAF(nEHVR*VH_bR) is the close-to-exact observed nonlinear site amplification factor. The nEHVR is the H/V ratio of an individual strong motion. The VH_bR is the same as that utilized in the linear case.

The npHSAF(nEHVR*VACF) is a nonlinear pseudo horizontal site amplification factor. The nEHVR is the H/V ratio of an individual strong motion. The VACF is the same as that utilized in the linear case.

The npHSAF(EHVR*VACF*NCF) is another nonlinear pseudo horizontal site amplification factor. The spectra from EHVR*NCF is the npEHVR (Nonlinear pseudo-EHVR) based on the NCF defined in Fig. 7 and 8.

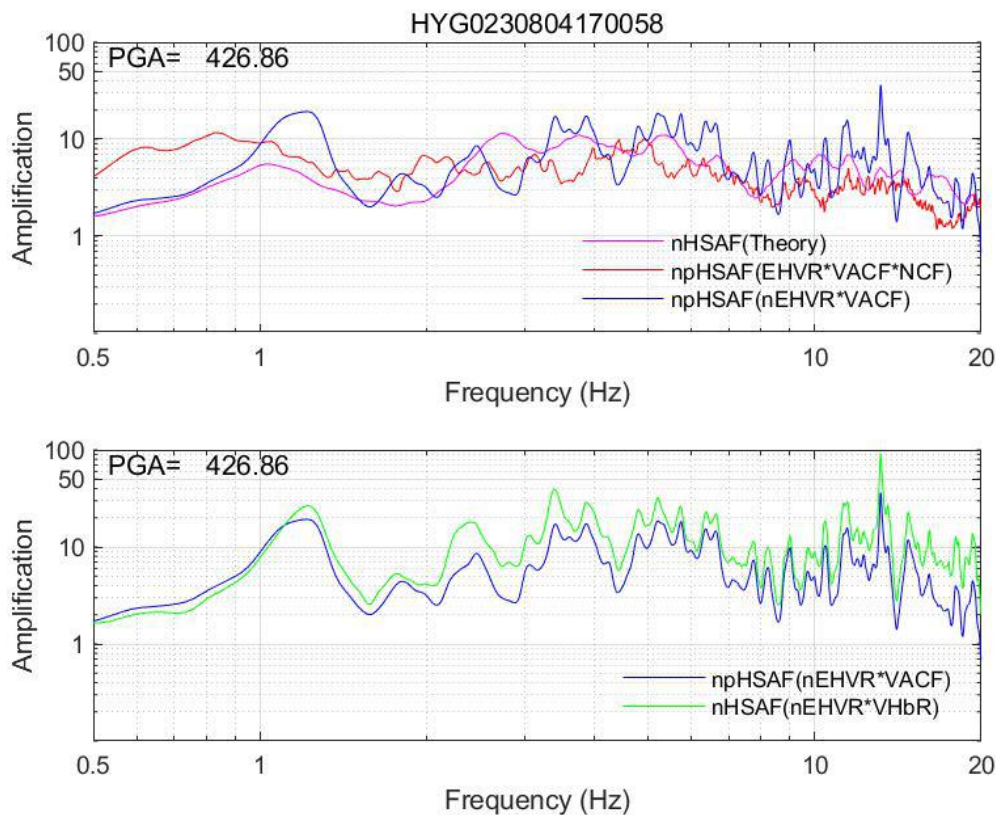


Fig. 14 – nHSAF(Theory), npHSAF(EHVR*VACF*NCF), nHSAF (nEHVR*VH_bR), and npHSAF(nEHVR*VACF) at HYG023.

Firstly, although the fluctuations on the nHSAF(nEHVR*VH_bR) and the npHSAF(nEHVR*VACF) in the lower panel are large relatively since they were calculated from an individual strong motion, we noted that three types of nHSAF in the upper panel are extremely similar in the overall tendency of descend and ascend. In the meantime, the matching of peak frequencies and their amplitudes is good, although it is not perfect.

Secondly, the similarity between the nHSAF(nEHVR*VH_bR) with the npHSAF (nEHVR*VACF) shows a reasonable practicability of the effective VACF method again.

Besides, the nHSAF(nEHVR*VH_bR) is the close-to-exact observed nonlinear site amplification factor, and the npHSAF(nEHVR*VACF) is a nonlinear empirical site amplification factor calculated by the effective and appropriate VACF method, they are powerful and practical as long as we have the observed strong motions with high PGAs. However, in the high PGA case for the seismic prediction, if we want to know an average level of the amplification at one site, the npHSAF(EHVR*VACF*NCF) is the only empirical way to get HSAF since the npHSAF(EHVR*VACF*NCF) can be obtained from observed data in the linear regime.

5. Conclusion

We have investigated observed strong motion data focusing our attention on the nonlinear characteristics that emerged in the observed EHVRs with high peak ground acceleration. Our empirical model to predict horizontal site amplification factors from EHVR, which accounts for both linear vertical amplification and nonlinear horizontal variation from the linear amplification, was found to be quite effective within a



reasonable range of nonlinearity. We need to extend our research to the data with much stronger nonlinearity, and to the reproduction of waveforms.

Acknowledgements

About the programs utilized in this paper, the program for velocity inversions is from Dr. Fumiaki Nagashima in DPRI, Kyoto University [3]. The program for the calculation of theoretical HSAF is DYNEQ, developed by Prof. Nozomu Yoshida [5]. Matlab programs made primarily by the first author were used on the calculation of EHVRs, DoD, NCF, and the image processing, we would like to thank all the members of Kawase Lab and Nishino Lab, including Mr. Okada and Ms. Doi of DPRI for their assistance.

References

- [1] Nakamura Y (1989): A method for dynamic characteristics of estimation of subsurface using microtremor on the ground, *Quarterly Report of RTEI*.
- [2] Noguchi S and Sasatani T (2011): Nonlinear soil response and its effects on strong ground motions during the 2003 Miyagi-Oki intraslab earthquakes, *Zishin* 2, 63, 165-187 (in Japanese with English abstract)
- [3] Nagashima F, Matsushima S, Kawase H, and Sanchez-Sesma, F J (2014): Application of Horizontal-to-Vertical Spectral Ratios of Earthquake Ground Motions to Identify Subsurface Structures at and around the K-NET Site in Tohoku, Japan, *Bulletin of the Seismological Society of America*, 104(5), 2288-2302.
- [4] Kawase H, F Nagashima, K Nakano, and Y Mori (2018): Direct evaluation of S-wave amplification factors from microtremor H/V ratios: Double empirical corrections to "Nakamura" method, *Soil Dyn. Earthq. Eng.*, Open Access.
- [5] Yoshida N and Suetomi I (1996): DYNEQ: A computer program for dynamic analysis of level ground based on equivalent linear method, *Reports of Engineering Research Institute*, Sato Kogyo Co Ltd, 61-70.
- [6] Shima E (1978): Seismic Microzoning map of Tokyo, *Proc. Second Inter. Conf. on Microzonation (1)*, 433-443.
- [7] Finn W D L (1991): Geotechnical engineering aspects of microzonation, *Proc. 4th International Conference on Seismic Zonation*, Vol.1, 199-259.
- [8] Kawase H and H Matsuo (2004): Amplification characteristics of K-NET, KiK-net, and JMA Shindokei network sites based on the spectral inversion technique, *13th World Conference on Earthquake*, Vancouver, Canada.
- [9] Kawase, H (2006): Site effects derived from spectral inversion method for K-NET and KiK-net and JMA strong-motion network with special reference to soil nonlinearity in high PGA records, *Bull. Earthq. Res. Inst. Univ. Tokyo*, 81,309-315.
- [10] K L Wen, T M Chang, C M Lin, and Chiang H J (2006): Identification of nonlinear site response during the 1999, Chi-Chi, Taiwan earthquake from the H/V spectral ratio, *Third International Symposium on the Effects of Surface Geology on Seismic Motion*, Grenoble, France.
- [11] Nakano K, S Matsushima, and H Kawase (2015): Statistical properties of strong ground motions from the generalized spectral inversion of data observed by K-NET, KiK-net, and the JMA Shindokei Network in Japan, *Bull. Seism. Soc. Am.*, 105, 2662-2680.
- [12] Nakano K, H Kawase, and S Matsushima (2019): A Study on the Site Amplifications Estimated by Generalized Inversion Technique, *J. Jpn. Assoc. Earthq. Eng.*, 19(2), 1-24. (In Japanese with English abstract)
- [13] Kawase H, E Ito, and K Nakano (2020): Direct Estimation of S-Wave Site Amplification Factors from Horizontal-To-Vertical Ratios of Earthquakes, 17th World Conference of Earthquake Engineering, September 13-18, Sendai, Japan, paper no. C000856.